



## Equilibrium, isotherm, and kinetic studies of zinc (II) adsorption onto natural hematite

Anahita Sattari<sup>a</sup>, Maryam Kavousi<sup>a</sup>, Mohammad Mehdi Salarirad<sup>a,\*</sup>, Haniyeh Jalayeri<sup>b</sup>

<sup>a</sup>Department of Mining and Metallurgical Engineering, Amirkabir University of Technology, Tehran, Iran, Tel. +98 6454 2974; email: [salari@aut.ac.ir](mailto:salari@aut.ac.ir) (M. Mehdi Salarirad)

<sup>b</sup>Department of Mining, Petroleum and Geophysics Engineering, Shahrood University of Technology, Shahrood, Iran

Received 11 January 2015; Accepted 28 August 2015

### ABSTRACT

In this study, natural hematite was used for the removal of zinc(II) from aqueous solutions due to its lower cost and high adsorption capacity. Variables of batch experiments including solution pH, contact time, initial concentration, and the amount of adsorbent were studied. The results indicated that the adsorption capacities are strongly affected by the parameters mentioned above. The optimum pH and amount of adsorbent was obtained 6 and 5 g, respectively. The isothermal data were fitted with Freundlich equation. The intraparticle diffusion model was the best for describing the kinetic data. It was revealed that natural hematite can be used as an effective adsorbent for removing Zn(II) from aqueous solutions.

*Keywords:* Natural hematite; Adsorption; Aqueous solution; Zinc(II)

### 1. Introduction

Zinc is widely used in industries such as galvanization, smelting, fertilizers and pesticides, fossil fuel combustion, pigment, polymer stabilizers, etc. and for this reason, there are large amount of wastewaters containing zinc. These industries directly or indirectly release large quantities of zinc in to environment, especially in developing countries [1,2]. Zinc is as an essential element for human health and acts as a micronutrient when present in trace amounts [3]. But it is reported that Zinc is toxic beyond 5 mg l<sup>-1</sup> according to World Health Organization (WHO) [4].

The undesirable effects of pollutants can be avoided or at least diminished by treatment of produced wastewater prior to discharge. Various methods have been employed for the removal of zinc, including

chemical precipitation, ion exchange, electroflotation, reverse osmosis, solvent extraction, electrolysis, and adsorption. Adsorption is one of the physicochemical treatment processes found to be effective in removing heavy metals from aqueous solutions [5]. Several adsorbents, most of them low cost and natural materials, have been reported for the adsorption of zinc from zinc-containing wastewaters, such as activated carbon [6–8], natural materials such as clay [9,10], zeolites [11,12], kaolinite [13], industrial wastes such as fly ash [14,15], coal, metal oxides [16], goethite [17–20], agricultural wastes such as maize leaf, sago waste, bush leaves, rice husk ash, and peanut hulls. [5]. Removal by adsorption can be cost-effective using recovery and reuse of conventional adsorbents like activated carbon [21], but the high cost of activated carbon has inspired the investigators especially in developing countries to search for suitable low-cost adsorbents [3]. Among the oxide minerals with local availability, especially

\*Corresponding author.

hematite and goethite are cheap materials compared with other adsorptive materials which have a large specific surface area and high adsorption capacity [22]. Synthetic and natural are usual kinds of hematite used for the adsorption of zinc. Recently, the use of natural hematite for adsorbing metal cations from aqueous solution attracted the attention of researchers [23]. Actually, the plethora of hematite and its cheapness make it a considerable substitution for costly adsorbents such as activated carbon. Furthermore, using hematite is the suitable alternative for avoiding regeneration processes, as regeneration processes are expensive, so it is beneficial to find such adsorbents that reduce the cost of the adsorption procedure. Hematite is low-cost adsorbent as well as is plentiful in Anguran region. So there is no need for regeneration process.

In the present study, we have used natural hematite as an adsorbent for zinc removal. In spite of high adsorption capacity for hematite and the economic benefits in supplying hematite as an adsorbent, there are few studies on using hematite as an adsorbent in the literature. This research has tried to prove the great application of natural hematite in the adsorption process with respect to its overabundance in nature and low cost. The natural hematite that was used in this study was from the Anguran mine, southwest of city of Zanjan. The lead and zinc beneficiation plant at Dandi with a capacity of about 140 tons per hour is located 100 km southwest of Zanjan town. Obviously, the concentration of zinc in the wastewater produced from this mining site is high. Zinc, as a heavy metal, has undesirable effects on local environment. Regarding that the zinc could be the best choice for this research, so has been used as an adsorbate in experiments.

In this paper, the behavior of the natural hematite in the batch process of adsorption in addition to its kinetics, and equilibrium isotherms were studied in order to optimize and design an adsorption process as well as adsorbent and adsorbate. The major parameters affecting the adsorption efficiency including the initial zinc concentration, pH, the amount of adsorbent, and contact time was investigated. The hematite particles characteristics before and after loading with zinc were studied with FTIR analysis and scanning electron microscope (SEM), and maps of zinc(II) distribution on the surface and inside the particles were prepared in order to evaluate the mechanism and distribution pattern of adsorbed zinc.

## 2. Materials and methods

### 2.1. Reagents

Zinc sulfate heptahydrate was purchased from Merck Company. A high-grade hematite was obtained

from Anguran, Zanjan, Iran, and then crushed to obtain lower particle sizes. Eventually, granular hematite was sieved to particle size of 150 micron. Acid treatment of hematite was employed with hydrochloric acid solution (1 M) to remove impurities present in hematite, and washed with distilled water, dried in the air, and then added to zinc solution of predetermined initial concentration.

### 2.2. Main instruments analytical methods

Mettler Toledo precision pH meters, X-ray diffraction (XRD) of hematite using BrukerD8 ADVANCE X-Ray diffractometer, and the atomic adsorption spectroscopy (AAS) for analyzing the concentration of zinc (II) ion were used in the experiments. Distribution maps of zinc were obtained through imaging with backscattered electrons (BSE) using a Philips XL30 SEM. Information about morphology and surface topography of hematite samples was obtained through imaging with secondary electrons (SE).

### 2.3. Batch equilibrium experiments

Adsorption tests were carried out using a 2.5 L capacity glass bottles at ambient temperature ( $25 \pm 2^\circ\text{C}$ ). Stock solution of zinc at the concentration of  $70 \text{ mg l}^{-1}$  was prepared by dissolving 0.3 g of zinc sulfate in 1 L of distilled water preadjusted to pH 4. Experimental solutions at desired concentration were obtained by dilution of the stock solution with distilled water preadjusted to pH 4. Stock solution at the concentration of  $70 \text{ mg l}^{-1}$  was also prepared, preadjusted to pH 2, 4, and 6 in order to determine an optimum pH for adsorption. The zinc(II) concentration of each solution was analyzed by titrating against EDTA solution in the presence of Erichrome black T as an indicator in order to check the values that were obtained from AAS. Five hundred milliliters of experimental solutions with initial concentration of  $70 \text{ mg l}^{-1}$  were placed in four bottles and then 2, 3, 4, and 5 g prepared hematite was added to each bottle. Bottles were rolled at a constant rotation of 100 rpm for 50 h to reach the equilibrium.

Sampling was performed by removing 10 mL aliquots at predetermined time intervals. Samples were then analyzed for zinc as above mentioned method. The amount of adsorption at equilibrium  $q_e$  ( $\text{mg l}^{-1}$ ) was calculated by Eq. (1):

$$q_e = \frac{(C_0 - C_e)V}{W} \quad (1)$$

where  $C_0$  and  $C_e$  ( $\text{mg l}^{-1}$ ) are initial ( $t = 0$ ) and equilibrium zinc concentrations, respectively.  $V$  is the volume of the solution (L), and  $W$  is the mass of dry hematite used (g).

#### 2.4. Batch kinetic experiments

Batch kinetic experiments were conducted under similar conditions mentioned above for equilibrium experiments. Experiments were performed at ambient temperature using 5 g of prepared hematite with 500 mL of aqueous zinc solutions in 2.5 L glass bottles with initial zinc concentrations of 70, 150  $\text{mg l}^{-1}$  and pH 4. Contents were rolled at 100 rpm by bottle roll apparatus. Sampling was done at regular time intervals and the concentration of zinc was measured as mentioned previously. The amount of zinc adsorbed by hematite at time  $t$ ,  $q_t$  ( $\text{mg l}^{-1}$ ), was calculated according to Eq. (2):

$$q_t = \frac{(C_0 - C_t)V}{W} \quad (2)$$

where  $C_t$  ( $\text{mg l}^{-1}$ ) is the zinc concentration at time  $t$ .

The adsorption rates could be calculated according to Eq. (3):

$$\text{adsorption (\%)} = \frac{C_0 - C_t}{C_0} \times 100\% \quad (3)$$

#### 2.5. Validity of kinetic model

In addition to correlation coefficient ( $R^2$ ), the kinetic models were further validated by the average relative error (ARE), which are defined as Eq. (4):

$$\text{ARE} = \frac{100}{N} \sum_{i=1}^N \left| \frac{q_e^{\text{exp}} - q_e^{\text{cal}}}{q_e^{\text{exp}}} \right|_i \quad (4)$$

where  $q_e^{\text{exp}}$  and  $q_e^{\text{cal}}$  ( $\text{mg l}^{-1}$ ) are experimental and calculated amount of zinc adsorbed on hematite at time  $t$ , and  $N$  is the number of measurements made. Models with lower ARE values show more accurate estimation of  $q_t$  values [24].

### 3. Results and discussion

#### 3.1. Characteristic of hematite

Fig. 1 displays the XRD of hematite with the particle size of about 150 micron. It is also specified that the crystal lattice of natural hematite is rhombohedral with the calculated density of  $5.2 \text{ g/cm}^3$  and cell volume of  $300.79 (10^6 \text{ pm}^3)$ . The structure of hematite is made up of hcp arrays of oxygen ions arranged in the  $[001]$  direction. Fe(III) ions are set out with two filled sites being followed by one vacant site  $(001)$  plane.

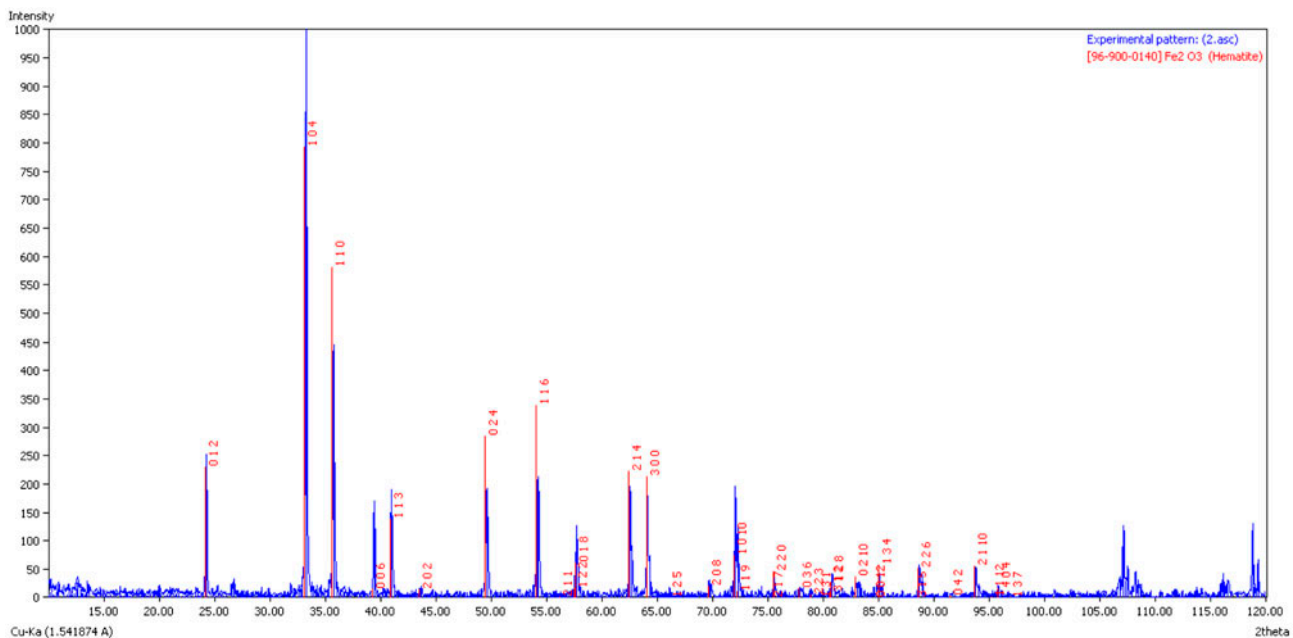


Fig. 1. XRD pattern of hematite.

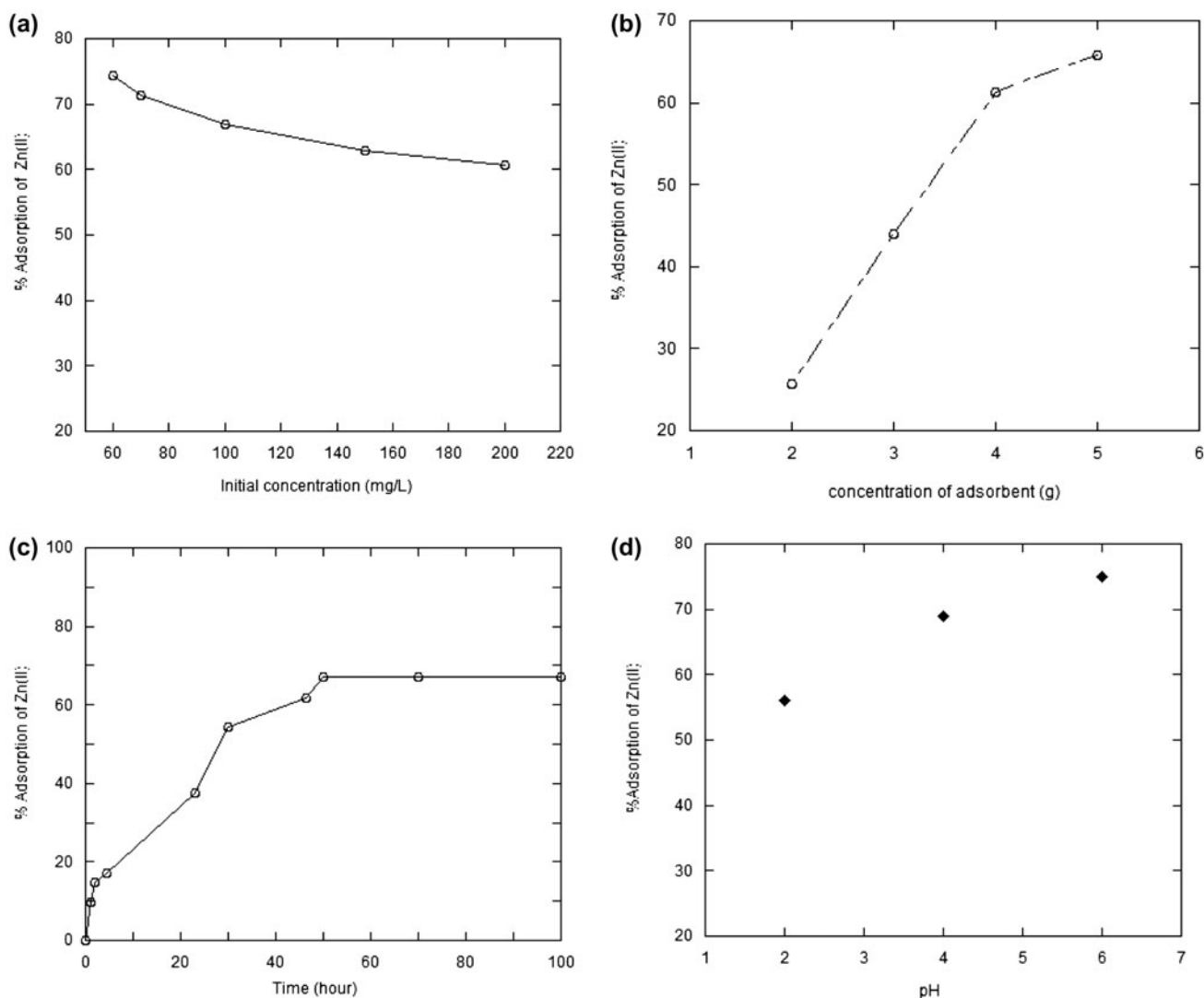


Fig. 2. (a) Effect of initial concentration on adsorption, (b) effect of concentration of adsorbent on adsorption, (c) effect of contact time on adsorption, and (d) effect of pH on adsorption.

### 3.2. Effect of initial concentration and the amount of adsorbent

The removal of Zn(II) was dependent on the initial concentration. As it is shown in Fig. 2(a), the amount of Zn(II) adsorbed  $q_e$  ( $\text{mg l}^{-1}$ ), increased with the increase in initial concentration. The ratio of available surface to initial Zn(II) concentration, at lower concentration was larger. Therefore, the adsorption became independent of initial concentration. Then, the percentage of adsorption at higher concentrations depended upon the initial concentration. In the case of natural hematite, the Zn(II) removal decreased from

74.33 to 60.76% with increasing Zn(II) concentration from 60 to 200  $\text{mg l}^{-1}$ , and the amount of  $q_e$  increased from 4.46 to 12.15  $\text{mg l}^{-1}$ .

The effect of adsorbent concentration on adsorbent capacity also was studied using 2, 3, 4, and 5 g of adsorbent with the fixed initial concentration of 70 ( $\text{mg l}^{-1}$ ) at ambient temperature and pH 4 are shown in Fig. 2(b). According to the results, the percentage of adsorption increased from 25.71 to 65.87% with increasing adsorbent concentration. This may be due to an increase in the number of adsorption sites on the surface of hematite [25].

Table 1  
Isotherms and their linearized expressions

Isotherms	Equations	Linear expression	Plot	Parameters	Refs.
Freundlich	$q_e = K_F (C_e)^{1/n}$	$\ln q_e = \ln K_F + n^{-1} \ln C_e$	$\ln q_e$ vs. $\ln C_e$	$K_F = \exp(\text{intercept})$ , $n = (\text{slope})^{-1}$	[28]
Langmuir	$q_e = (q_m K_L C_e) / (1 + K_L C_e)$	Type (I) $C_e/q_e = (1/K_L q_m) + (C_e/q_m)$ Type (II) $1/q_e = (1/K_L q_m C_e) + (1/q_m)$	$C_e/q_e$ vs. $C_e$ $1/q_e$ vs. $1/C_e$	$q_m = (\text{slope})^{-1}$ , $K_L = \text{slope}/\text{intercept}$ $q_m = (\text{intercept})^{-1}$ , $K_L = \text{intercept}/\text{slope}$	[29]
Temkin	$q_e = q_m \ln (K_T C_e)$	Type (III) $q_e = q_m - (1/K_L) q_e / C_e$	$q_e$ vs. $q_e / C_e$	$q_m = \text{intercept}$ , $K_L = -(\text{slope})^{-1}$	
Dubinin–Radushkevich	$q_e = q_m \exp(-D \epsilon^2)$ $\epsilon = RT \ln(1 + C_e^{-1})$	Type (IV) $q_e / C_e = K_L q_m - K_L q_e$ $q_e = q_m \ln K_T + q_m \ln C_e$ $\ln q_e = \ln q_m - D \epsilon^2$	$q_e / C_e$ vs. $q_e$ $q_e$ vs. $\ln C_e$ $\ln q_e$ vs. $\epsilon^2$	$q_m = -(\text{intercept}/\text{slope})$ , $K_L = -\text{slope}$ $q_m = \text{slope}$ , $K_T = \exp(\text{intercept}/\text{slope})$ $q_m = \exp(\text{intercept})$ , $D = -\text{slope}$	[30] [31]

Table 2  
Isothermal parameters for the sorption of zinc(II) by hematite

$q_e/C_e$	$1/C_e$	$1/q_e$	$\ln(q_e)$	$\ln(C_e)$	$C_e$ (mg l <sup>-1</sup> )	$q_e$ (mg g <sup>-1</sup> )
0.28961	0.064935	0.224215	1.495149	2.734368	15.4	4.46
0.248259	0.049751	0.200401	1.607436	3.00072	20.1	4.99
0.169542	0.026954	0.158983	1.838961	3.613617	37.1	6.29
0.201811	0.020121	0.099701	2.305581	3.906005	49.7	10.03
0.154842	0.012742	0.082291	2.497494	4.362844	78.48	12.152

Table 3  
Kinetic models parameters by linear regression method for the sorption of zinc(II) by hematit

Isotherms	$R^2$	Parameters
Freundlich	0.9431	$\ln(q_e)$ vs. $\ln(C_e)$
Langmuir (type I)	0.7542	$C_e/q_e$ vs. $C_e$
Langmuir (type II)	0.921	$1/q_e$ vs. $1/C_e$
Langmuir (type III)	0.5722	$q_e$ vs. $q_e/C_e$
Langmuir (type IV)	0.5722	$q_e/C_e$ vs. $q_e$
Temkin	0.9091	$q_e$ vs. $\ln(C_e)$

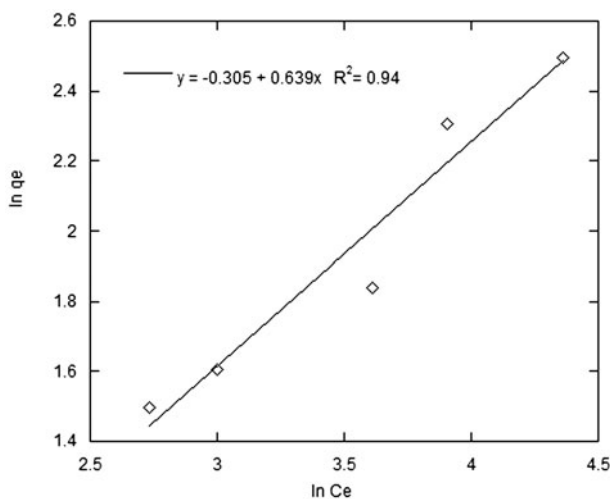


Fig. 3. Adsorption isotherm at Zn(II) adsorbed on natural hematite.

### 3.3. Effect of contact time on adsorption

In order to determine the optimum adsorption time for hematite used in this study, the effect of contact time on adsorption was determined at 298 k using the stock solution which has the zinc ion concentration of 70 (mg l<sup>-1</sup>). As it can be seen from Fig. 2(c), the zinc removal increased rapidly at the beginning of adsorption with increase in contact time, and thereafter attained to the equilibrium, and became almost

constant after equilibrium point. This result is based on the fact that a large number of sites are available for adsorption at the beginning of the process, and few minutes later, the remaining vacant surface sites are hard to be occupied because of the forces between the Zn(II) and the aqueous phases [25]. Results showed that the equilibrium reached at 52 h for natural hematite.

### 3.4. Effect of initial pH on adsorption

The results given in Fig. 2(d) indicate that the adsorption values of the hematite are clearly pH dependent and increased with increasing pH value from 2 to 6. At used pH range, zinc is only present as a dissolved metal [26]. While for pH values above 6, the zinc may precipitate as ZnOH, and Zn(OH)<sub>2</sub>. Accordingly, the percentage of adsorption is decreased.

### 3.5. Equilibrium isotherms

Adsorption isotherm is the most important parameter for the design of adsorption systems since they represent how the metal ions are partitioned between the adsorbent and liquid phases at equilibrium as a function of metal ion concentration [22]. Many isotherm models have been proposed to analyze the adsorption equilibrium data. The equilibrium sorption data could be fitted into Langmuir, Freundlich, and Temkin isotherms. Isotherm models and their linearized expressions are listed in Table 1. Tables 2 and 3 represent the values of isothermal parameters and correlation coefficients ( $R^2$ ) of different isotherm models for adsorption of zinc(II) onto hematite. Based on Fig. 3, and the values of  $R^2$ , the adsorption pattern of zinc by natural hematite is in accordance with the Freundlich isotherms.

Freundlich model is an empirical model that can be applied to multilayer adsorption, and is used widely in heterogeneous systems [27]. The Freundlich equation is given by Eq. (5):

Table 4  
Kinetic models and their linearized expression

Kinetic models	Equations	Linear expression	Plot	Parameters	Refs.
Elovich	$q_t = \beta \ln(\alpha\beta t)$	$q_t = \beta \ln(\alpha\beta) + \beta \ln t$	$q_t$ vs. $\ln t$	$\beta = \text{slope}, \alpha = (\text{slope})^{-1} \exp(\text{intercept}/\text{slope})$	[37]
Zero order	$q_t = q_e - k_0 t$	$q_t = q_e - k_0 t$	$q_t$ vs. $t$	$q_e = \text{intercept}, k_0 = -(\text{slope})$	[38]
First order	$q_e = q_t \exp(k_1 t)$	$\ln(q_e/q_t) = k_1 t$	$\ln(q_t)$ vs. $t$	$q_e = \text{intercept}, k_1 = -(\text{slope})$	[38]
Pseudo-first-order	$q_t = q_e [1 - \exp(-k_{1p} t)]$	$\ln(q_e - q_t) = \ln q_e - k_{1p} t$	$\ln(q_e - q_t)$ vs. $t$	$q_e = \exp(\text{intercept}), k_{1p} = -(\text{slope})$	[39]
Second order	$q_t = q_t/(1 + q_e k_2 t)$	$q_t^{-1} = q_e^{-1} + k_2 t$	$q_t^{-1}$ vs. $t$	$q_e = (\text{intercept})^{-1}, k_2 = \text{slope}$	[40]
Pseudo-second-order	$q_t = k_{2p} q_e^2 t / (1 + q_e k_{2p} t)$	Type(I) $t/q_t = 1/k_{2p} q_e^2 + t/q_e$	$t/q_t$ vs. $t$	$q_e = \text{slope}^{-1}, k_{2p} = (\text{slope}^2)/\text{intercept}$	[41]
Intraparticle diffusion	$q_t = k_p t^{0.5}$	Type(II) $1/q_t = (1/k_{2p} q_e^2)(1/t) + (1/q_e)$	$1/q_t$ vs. $1/t$	$q_e = \text{intercept}^{-1}, k_{2p} = (\text{intercept}^2)/\text{slope}$	[42]
		Type(III) $q_t = q_e - (1/k_{2p} q_e) q_t/t$	$q_t$ vs. $q_t/t$	$q_e = \text{intercept}, k_{2p} = -1/(\text{slope} \times \text{intercept})$	
		Type(IV) $q_t/t = k_{2p} q_e^2 - k_{2p} q_e q_t$	$q_t/t$ vs. $q_t$	$q_e = -\text{intercept}/\text{slope}, k_{2p} = (\text{slope}^2)/\text{intercept}$	
			$q_t$ vs. $t^{0.5}$	$k_s = \text{slope}$	

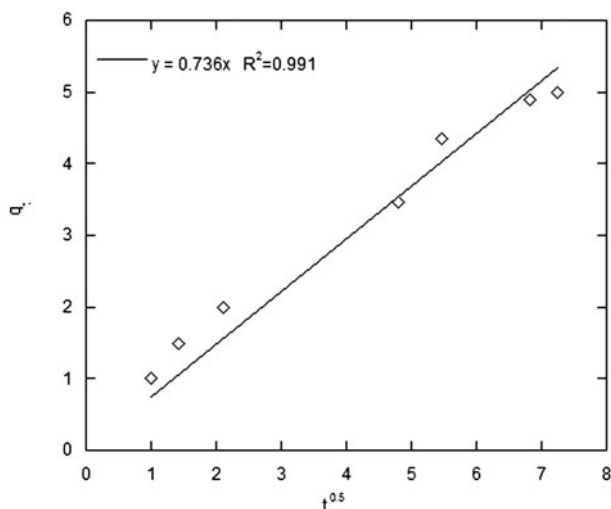


Fig. 4. Intraparticle diffusion adsorption kinetics of Zn(II) on natural hematite.

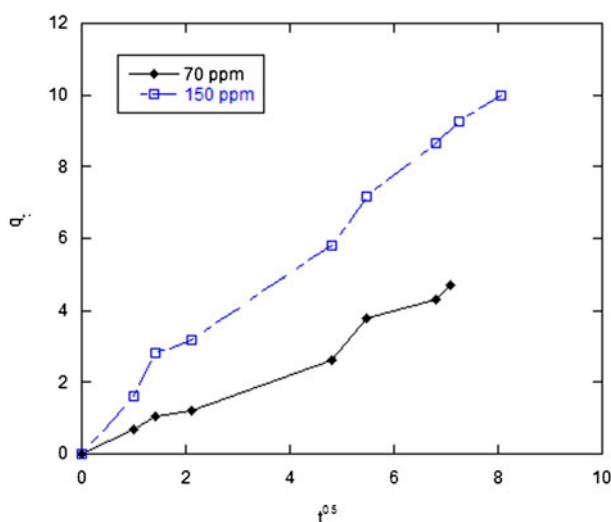


Fig. 5. Intraparticle diffusion adsorption kinetics of Zn(II) on natural hematite with the initial concentration of 70 and 150 ppm.

$$q_e = K_F(C_e)^{1/n} \tag{5}$$

Eq. (6) can also be transformed into linear form:

$$\ln q_e = \ln K_F + n^{-1} \ln C_e \tag{6}$$

Values  $K_F$  and  $1/n$  are Freundlich constants related to adsorption capacity and intensity of adsorption or surface heterogeneity, respectively. The slope ranges

between 0 and 1, becoming more heterogeneous as its value gets closer to zero.

### 3.6. Kinetics of zinc(II) adsorption by natural hematite

Adsorption mechanism mainly consists of three steps: (i) mass transfer through the external boundary layer film of liquid surrounding the outside of the particle; (ii) adsorption at site on the adsorbent particle surface; this step is often considered to be highly rapid; (iii) diffusion of adsorbate molecules to an adsorption site [32].

In this study, the zero-order kinetic model, Elovich kinetic model, first-order kinetic model, second-order kinetic model, pseudo-first-order kinetic model, pseudo-second-order kinetic model, and intraparticle diffusion model were employed to describe the kinetic characteristics of zinc adsorbed by hematite, and the parameters of adsorption kinetic models were calculated. Kinetic models and their linearized expressions are listed in Table 4.

Intraparticle diffusion model fitted the data better than other kinetic models as shown in Fig. 4.

Weber and Morris had showed the rate constant for intraparticle diffusion in 1962 by Eq. (7):

$$q_t = k_{id}t^{1/2} \tag{7}$$

where  $q_t$  is the amount of adsorption ( $\text{mg g}^{-1}$ ) at time  $t$  (h) [33,34]. According to Weber and Morris, the plot of  $q_t$  (the amount of adsorption at any time) against  $t^{1/2}$  would be linear that is forced to pass through the origin. Fig. 5 indicates that the curve is followed by a linear portion and plateau. The linear portion which was sharp was attributed to the diffusion of zinc ions through the solution to the external surface of the adsorbent where intraparticle diffusion was rate controlling. The plateau was attributed to the equilibrium, where intraparticle diffusion started to slow down due to the extremely low zinc concentration left in the solution [32,35]. It can be inferred that the diffusion in bulk phase to the outer surface of adsorbent is the fastest step. The value of rate constant ( $k_{id}$ ) was obtained from the slope of the linear portion of the curve.

The values of correlation coefficients ( $R^2$ ), ARE and constants of different kinetic models for sorption of zinc(II) onto hematite are shown in Table 5. Low correlation coefficients, and high ARE approve that Elovich, zero-order, first-order, pseudo-first-order, second-order, and pseudo-second order are not appropriate models.

Table 5

Kinetic models parameters by linear regression method for the adsorption of zinc(II) by hematite

Kinetic models	$R^2$	ARE	Parameters
Elovich	0.9153	23.66	$\alpha = 1.29203 \text{ mg g}^{-1} \text{ h}^{-1}$ ; $\beta = 1.0034 \text{ g mg}^{-1}$
Zero order	0.8892	39.39	$k_0 = -0.1011 \text{ mg g}^{-1} \text{ h}^{-1}$ ; $q_e = 0 \text{ mg g}^{-1}$
First order	0.9073	19.37	$q_e = 0.068 \text{ mg g}^{-1}$ ; $k_1 = -0.0358 \text{ h}^{-1}$
Pseudo-first-order	0.964	40.49	$q_e = 4.5267 \text{ mg g}^{-1}$ ; $k_{1p} = 0.0507 \text{ h}^{-1}$
Second order	0.7614	70.36	$q_e = 0.9276 \text{ mg g}^{-1}$ ; $k_2 = -0.0203 \text{ g mg}^{-1} \text{ h}^{-1}$
Pseudo-second-order Type(I)	0.9122	18.26	$q_e = 5.11509 \text{ mg g}^{-1}$ ; $k_{2p} = 0.0229 \text{ g mg}^{-1} \text{ h}^{-1}$
Pseudo-second order Type(II)	0.9288	20.83	$q_e = 3.4281 \text{ mg g}^{-1}$ ; $k_{2p} = 0.0674 \text{ g mg}^{-1} \text{ h}^{-1}$
Pseudo-second-order Type(III)	0.9097	86.99	$q_e = 0.0398 \text{ mg g}^{-1}$ ; $k_{2p} = 62.08 \text{ g mg}^{-1} \text{ h}^{-1}$
Intraparticle diffusion	0.991	9.085	$k_p = 0.6421 \text{ mg g}^{-1} \text{ h}^{-0.5}$

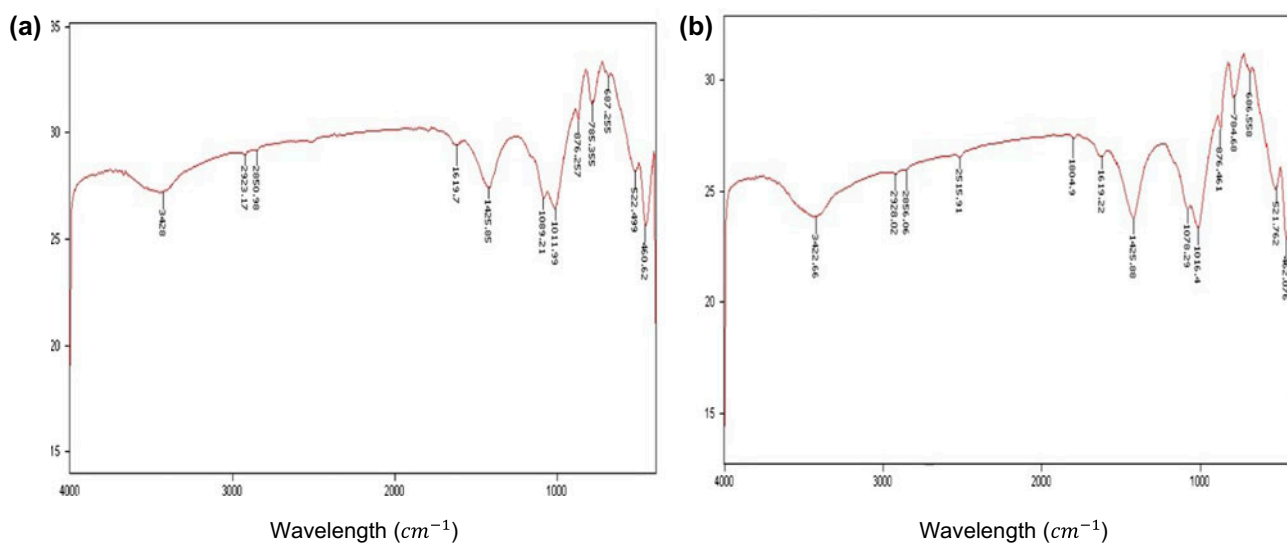


Fig. 6. IR spectra of powder hematite (a) before, and (b) after adsorption.

The correlation coefficient ( $R^2$ ) and ARE for intraparticle diffusion model were 0.991 and 9.085%, respectively. These values greatly demonstrate that the sorption of zinc(II) onto natural hematite is described by intraparticle diffusion model.

The calculated  $k_p$  for the initial concentration of 70 ppm was  $0.736 \text{ mg g}^{-1} \text{ h}^{-0.5}$  and for 150 ppm was  $1.1547 \text{ mg g}^{-1} \text{ h}^{-0.5}$ . It can be concluded by Fig. 5 that an increase in initial concentration leads to an increase in the rate parameter. This may be due to the fact that the intraparticle diffusion model obeys Fick's law. A further concentration gradient resulted in faster diffusion and quicker adsorption [32]. It is claimed that, Fick's diffusion model is one of the simplest approaches for the description of adsorption in terms of rate coefficients, while internal diffusion steps control the process. Eq. (8) as a kinetic equation was obtained from Fick's diffusion model [36]:

$$\frac{q_t}{q_e} = 1 - \frac{6}{\pi^2} \sum_{n=1}^{\infty} \frac{1}{n^2} \exp\left(-\frac{n^2 \pi^2 D_{\text{eff}} t}{R_p^2}\right) \quad (8)$$

### 3.7. FTIR analysis

The FTIR spectra of powder hematite, before and after adsorption are shown in Figure. The results obtained from the spectra are explained as follows. Fig. 6 represents the hematite's IR spectra before after adsorption. Some of the peaks that can be identified from IR spectra of hematite are as follows: the band at around  $3400 \text{ cm}^{-1}$  corresponds to O–H, the adsorption bands at around  $950$  and  $630 \text{ cm}^{-1}$  are attributed to hydroxyl groups at the IR spectrum of hematite. One of the peaks that have appeared in the spectra of hematite after adsorption is S–H band at  $2510 \text{ cm}^{-1}$ ,

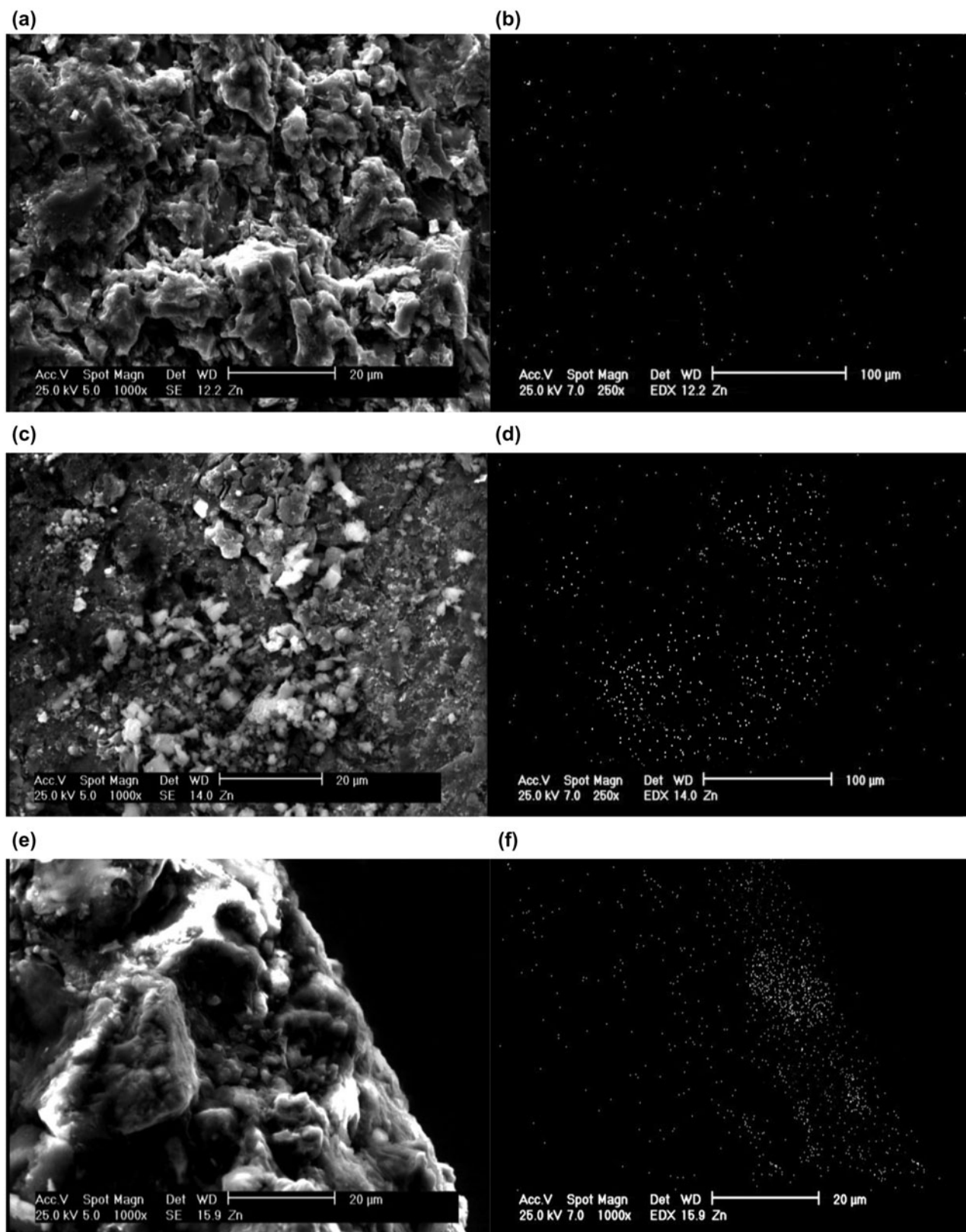


Fig. 7. (a) SEM micrograph of hematite before adsorption, (b) map of distribution of zinc before adsorption, (c) SEM micrograph of external surface of hematite after adsorption, (d) map of distribution of zinc after adsorption, (e) SEM micrograph of incised surface of hematite after adsorption, and (f) map of distribution of zinc after adsorption.

which refers to the addition of zinc sulfate to the aqueous solution [43,44].

### 3.8. SEM analysis

Fig. 7(a) and (b) show the surface morphology of external surface of hematite and the map of distribution of zinc, respectively, before adsorption. As might be expected, there is a limited amount of zinc distributed on the surface of hematite. In the same way, Fig. 7(c) and (d) represent the surface morphology of external surface of hematite and the map of distribution of zinc, respectively, after adsorption. Hematite sample after adsorption was cut into two parts, and Fig. 7(e) demonstrates a cross section of two broken hematite after adsorption of Zn(II) ions, and the map of distribution of zinc ion over the scanned area was presented in Fig. 7(f), as well. It can be seen that the distribution of zinc decreases by increasing the distance from surface toward interior parts of the hematite, and the distribution of zinc on the external surface of the hematite is high. Thus, the comparison of images in the following figures reveals that the intraparticle diffusion model is appropriate to describe the adsorption process of Zn(II) by hematite. It can be concluded that the transfer of zinc ions from the solution through the particle–solution interface, into the pores of the particle as well as the adsorption on the available surface of adsorbent are both responsible for the uptake of zinc ions [27].

## 4. Conclusion

In this study, the adsorption of zinc(II) from aqueous solution onto natural hematite in a batch system was investigated. It can be realized from results that the adsorption capacity of natural hematite was influenced by pH, initial concentration of solution, adsorbent concentration, and contact time. The adsorption capacity increased with the increase in pH and at the pH around 6, the maximum adsorption was obtained. At the pH beyond 6, zinc may precipitate as ZnOH, and Zn(OH)<sub>2</sub>. Additionally, adsorbent dosage of 2, 3, 4 and 5 g was studied, and it was observed that optimum dose of adsorbent is 5 g, because of a large number of adsorption sites on the surface of hematite.

On the basis of the experimented data, the Freundlich isotherm model fitted the equation data better than other models. The kinetic data closely fitted intraparticle diffusion model, and percentage of an ARE and SEM analysis follow this model as well. It was also concluded that different initial concentrations can affect the kinetics of the process, as increasing in ini-

tial concentration causes an increase in rate parameter. This could be referred to the fact that the intraparticle diffusion model obeys Fick's law. Higher concentration gradient resulted in faster diffusion and quicker adsorption.

## Nomenclature

$K_F$	—	Freundlich constant ( $\text{mg g}^{-1} (\text{L/g})^{1/n}$ )
$1/n$	—	Freundlich exponent
$K_L$	—	Langmuir isotherm constant ( $\text{L mg}^{-1}$ )
$K_T$	—	Temkin isotherm constant ( $\text{L mg}^{-1}$ )
$D$	—	Dubinin–Redushkevich isotherm constant ( $\text{mol}^2 \text{kJ}^{-2}$ )
$k_0$	—	zero order kinetic model constant ( $\text{g mg}^{-1} \text{h}^{-1}$ )
$k_1$	—	first-order kinetic model constant ( $1/\text{h}$ )
$k_{1p}$	—	pseudo-first-order kinetic model constant ( $1/\text{h}$ )
$k_2$	—	second-order kinetic model constant ( $\text{g mg}^{-1} \text{h}^{-1}$ )
$k_{2p}$	—	pseudo-second-order kinetic model constant ( $\text{g mg}^{-1} \text{h}^{-1}$ )
$k_p$	—	intraparticle diffusion kinetic model constant ( $\text{g mg}^{-1} \text{h}^{-0.5}$ )
$R^2$	—	correlation coefficient
ARE	—	average relative error
$p$	—	number of parameters in isotherm
$N$	—	number of experimental measurements
$C_e$	—	equilibrium concentration ( $\text{mg l}^{-1}$ )
$C_0$	—	initial concentration ( $\text{mg l}^{-1}$ )
$C_t$	—	concentration at time $t$ ( $\text{mg l}^{-1}$ )
$q_e$	—	amount of zinc adsorbed at equilibrium ( $\text{mg g}^{-1}$ )
$q_m$	—	monolayer sorption capacity ( $\text{mg g}^{-1}$ )
$q_t$	—	amount of zinc adsorbed at time $t$ ( $\text{mg g}^{-1}$ )
$t$	—	time (h)
$V$	—	volume of the solution (L)
$W$	—	mass of natural hematite used (g)
<i>Greek letters</i>		
$\alpha$	—	Elovich kinetic model constant ( $\text{mg g}^{-1} \text{h}^{-1}$ )
$\beta$	—	Elovich kinetic model constant ( $\text{g mg}^{-1}$ )

## References

- [1] C. Gakwisiri, A critical review of removal of zinc from wastewater, Proceedings of the World Congress on Engineering, London, July 4–6, (2012).
- [2] F. Fu, Q. Wang, Removal of heavy metal ions from wastewaters: A review, J. Environ. Manage. 92 (2011) 407–418.

- [3] A.K. Bhattacharya, S.N. Mandal, S.K. Das, Adsorption of Zn(II) from aqueous solution by using different adsorbents, *Chem. Eng. J.* 123 (2006) 43–51.
- [4] M. Kumar, A. Puri, A review of permissible limits of drinking water, *Indian J. Occup. Environ. Med.* 16 (2012) 40–44.
- [5] W.S. Wan Ngah, M.A. Hanafiah, Removal of heavy metal ions from wastewater by chemically modified plant wastes as adsorbents: A review, *Bioresour. Technol.* 99 (2008) 3935–3948.
- [6] S. Babel, T.A. Kurniawan, Low-cost adsorbents for heavy metals uptake from contaminated water: A review, *J. Hazard. Mater.* 97 (2003) 219–243.
- [7] L. Monser, N. Adhoum, Modified activated carbon for the removal of copper, zinc, chromium and cyanide from wastewater, *Sep. Purif. Technol.* 26 (2002) 137–146.
- [8] R. Leyva Ramos, L.A. Bernal Jacome, J. Mendoza Barron, L. Fuentes Rubio, R.M. Guerrero Coronado, Adsorption of zinc(II) from an aqueous solution onto activated carbon, *J. Hazard. Mater.* 90 (2002) 27–38.
- [9] T. Vengris, R. Binkiene, A. Sveikauskaite, Nickel, copper and zinc removal from waste water by a modified clay sorbent, *Appl. Clay Sci.* 18 (2001) 183–190.
- [10] S. Veli, B. Alyüz, Adsorption of copper and zinc from aqueous solutions by using natural clay, *J. Hazard. Mater.* 149 (2007) 226–233.
- [11] A.M. El-Kamash, A.A. Zaki, M. Abdel-Geleel, Modeling batch kinetics and thermodynamics of zinc and cadmium ions removal from waste solutions using synthetic zeolite A, *J. Hazard. Mater.* 127 (2005) 211–220.
- [12] J. Perić, M. Trgo, N. Vukojević Medvidović, Removal of zinc, copper and lead by natural zeolite: A comparison of adsorption isotherms, *Water Res.* 38 (2004) 1893–1899.
- [13] K.G. Bhattacharyya, S.S. Gupta, Adsorption of a few heavy metals on natural and modified kaolinite and montmorillonite: A review, *Adv. Colloid Interface Sci.* 140 (2008) 114–131.
- [14] G. Gupta, N. Torres, Use of fly ash in reducing toxicity of and heavy metals in wastewater effluent, *J. Hazard. Mater.* 57 (1998) 243–248.
- [15] I. Alinnor, Adsorption of heavy metal ions from aqueous solution by fly ash, *Fuel* 86 (2007) 853–857.
- [16] S.K. Srivastava, G. Bhattacharjee, R. Tyagi, N. Pant, N. Pal, Studies on the removal of some toxic metal ions from aqueous solutions and industrial waste. Part I (Removal of lead and cadmium by hydrous iron and aluminum oxide), *Environ. Technol. Lett.* 7 (1998) 1173–1185.
- [17] P. Trivedi, L. Axe, J. Dyer, Adsorption of metal ions onto goethite: single-adsorbate and competitive systems, *Colloids Surf., A: Physicochem. Eng. Aspects* 191 (2001) 107–121.
- [18] Z.S. Kooner, Comparative study of adsorption behavior of copper, lead, and zinc onto goethite in aqueous systems, *Environ. Geol.* 21 (1998) 242–250.
- [19] N.J. Barrow, J. Gerth, G.W. Brümmer, Reaction kinetics of the adsorption and desorption of nickel, zinc and cadmium by goethite. II Modelling the extent and rate of reaction, *J. Soil Sci.* 40 (1989) 437–450.
- [20] E.A. Forbes, A.M. Posner, J.P. Quirk, The specific adsorption of divalent Cd, Co, Cu, Pb, and Zn on Goethite, *Appl. Geochem.* 22 (2007) 249–275.
- [21] D.B. Singh, D.C. Rupainwar, G. Prasad, K.C. Jayaprakas, Studies on the Cd(II) removal from water by adsorption, *J. Hazard. Mater.* 60 (1998) 29–40.
- [22] M.C. Duff, C. Amrhein, Uranium(VI) adsorption on goethite and soil in carbonate solutions, *Soil Sci. Soc. Am. J.* 60 (1996) 1393–1400.
- [23] R.M. Cornell, U. Schwertmann, *The Iron Oxides, Structure, Properties, Reactions, Occurrences and Uses*, second ed., Wiley-VCH GmbH & Co, KGaA, 2003.
- [24] A. Behnamfard, M.M. Salarirad, Equilibrium and kinetic studies on free cyanide adsorption from aqueous solution by activated carbon, *J. Hazard. Mater.* 170 (2009) 127–133.
- [25] R. Pandey, N.G. Ghazi Ansari, R.L. Lakhan Prasad, R.C. Chandra Murthy, Pb(II) removal from aqueous solution by *Cucumis sativus* (Cucumber) peel: Kinetic, equilibrium & thermodynamic study, *Am. J. Environ. Prot.* 2 (2014) 51–58.
- [26] D.M. Ayres, A.P. Davis, P.M. Gietka, *Removing Heavy Metals from Wastewater*, University of Maryland, August, 1994.
- [27] K.Y. Foo, B.H. Hameed, Insights into the modeling of adsorption isotherm systems, *Chem. Eng. J.* 156 (2010) 2–10.
- [28] H.M.F. Freundlich, Über die adsorption in losungen (Over the adsorption in solution), *Z. Phys. Chem. J.* 57 (1906) 385–470.
- [29] I. Langmuir, The adsorption of gases on plane surfaces of glass, mica and platinum *J. Am. Chem. Soc.* 40 (1918) 1361–1403.
- [30] M.J. Temkin, V. Pyzhev, Recent modifications to Langmuir isotherms, *Acta Phys. Chim. Sin.* 12 (1940) 217–222.
- [31] M.M. Dubinin, L.V. Radushkevich, The equation of the characteristic curve of the activated charcoal, *Proceeding of the USSR Academy of Sciences* 55 (1947) 331–337.
- [32] W.H. Cheung, Y.S. Szeto, G. McKay, Intraparticle diffusion processes during acid dye adsorption onto chitosan, *Bioresour. Technol.* 98 (2007) 2897–2904.
- [33] F.C. Wu, R.L. Tseng, R.S. Juang, Initial behavior of intraparticle diffusion model used in the description of adsorption kinetics, *Chem. Eng. J.* 153 (2009) 1–8.
- [34] C.K. Jain, Adsorption of zinc onto bed sediments of the River Ganga: Adsorption models and kinetics, *Hydrol. Sci. J.* 46 (2001) 419–434.
- [35] B. Yasamin, T. Zeki, Removal of heavy metals from aqueous solution by sawdust adsorption, *J. Environ. Sci.* 19 (2007) 160–166.
- [36] G. Skodras, I. Diamantopoulou, G. Pantoleonos, G.P. Sakellariopoulos, Kinetic studies of elemental mercury adsorption in activated carbon fixed bed reactor, *J. Hazard. Mater.* 158 (2008) 1–13.
- [37] M.J.D. Low, Kinetics of chemisorption of gases on solids, *Chem. Rev.* 60 (1960) 267–312.
- [38] Y. Khambhaty, K. Mody, S. Basha, B. Jha, Kinetics, equilibrium and thermodynamic studies on biosorption of hexavalent chromium by dead fungal biomass of marine *Aspergillus niger*, *Chem. Eng. J.* 145 (2009) 489–495.

- [39] S. Lagergren, About the theory of so-called adsorption of soluble substances, *K. Svenska vet. akad. handlingar*. 24 (1898) 1–39.
- [40] G.M. Xu, Z. Shi, J. Deng, Adsorption of antimony on IOCS: Kinetics and mechanisms, *Acta Sci. Circum.* 26 (2006) 607–612 (in Chinese).
- [41] Y.S. Ho, G. McKay, A comparison of chemisorption kinetic models applied to pollutant removal on various sorbents, *Process Saf. Environ. Prot.* 76 (1998) 332–340.
- [42] W.J. Weber, J.C. Morris, Kinetics of adsorption on carbon from solutions, *J. Sanit. Eng. Div. Am. Soc. Civ. Eng.* 89 (1963) 31–60.
- [43] J.L. Rendon, C.J. Serna, IR spectra of powder hematite: Effects of particle size and shape, *Clay Miner.* 16 (1981) 375–382.
- [44] Donald Pavia, Gary Lampman, George Kriz, James Vyvyan, *Introduction to Spectroscopy*, fourth ed., Cengage Learning, 2008.